CHEMICAL ENGINEERING TRANSACTIONS
VOL. 94, 2022
A publication of AIDIC
The Italian Association of Chemical Engineering
Online at www.cetjournal.it
Guest Editors: Petar S. Varbanov, Yee Van Fan, Jiří J. Klemeš, Sandro Nižetić

ISBN 978-88-95608-93-8; **ISSN** 2283-9216
DOI: 10.3303/CET2294237

Synthesis and Characterization of Graphene-doped Nanofibrous Scaffolds for Tissue Engineering

Ana M. Muñoz-Gonzalez[a], Dianney Clavijo-Grimaldo[a,b,*]

[a] Universidad Nacional de Colombia, Carrera 45 # 26 – 85, Bogotá Colombia.
[b] Fundación Universitaria Sanitas, Calle 22B # 66-46, Bogotá Colombia
dclavijog@gmail.com

Graphene is a promising reinforced material used in a vasty of applications due its high mechanical resistance, high electrical and thermal conductivity. These properties could improve the electrical conductivity and mechanical properties of polymeric nanofibers. Nervous, muscular, and cardiac tissues are a challenge for Tissue Engineering not only because of their poor regeneration but because conventional, non-conductive scaffolds are unable to establish an adequate electromechanical coupling. In the present work, graphene was investigated as a nanofiller in a muti-layered polymer scaffold manufactured by electrospinning. The graphene-doped scaffolds were characterized to prospect their use in tissue engineering.

1. Introduction

Graphene is a promising reinforcement materials for potential applications such as flexible solar panels, batteries and capacitors, sensors, imaging, nanoelectronics, and tissue engineering (Ahadian et al., 2016). Furthermore, graphene has an outstanding mechanical resistance, electrical and thermal conductivity (Randviir et al., 2014). Additionally, the honeycomb structures, strong carbon-carbon bonding, elasticity, large specific surface area, and the ability to absorb biomolecules, cells, and tissues, make graphene suitable and practical for tissue engineering (Heidari et al., 2019).

Tissue engineering conflates the engineering and life science to restore the function of damaged tissues using biomaterials. One of the most versatile, promising, and cost-effective method for fabricating nanofibers from a variety of polymers used in tissue engineering is electrospinning. Electrospinning scaffolds are capable of mimic the fibrous structure of the extracellular matrix (ECM) (Xue et al., 2019). Nanofibers are generated by the application of an electric field to an injected solution. In this technique, when the electrostatic forces overcome solution surface tension, an accelerated jet arrives at the collector (target) after the formation of a Taylor cone (Chem et al., 2021).

Despite the current solutions for tissue engineering, some biomaterials lack in their electrical conductivity (Qasim et al., 2019), and mechanical properties, both relevant to stimulate the adhesion, spreading, and proliferation of cells. For example, conductivity is crucial for cardiomyocytes in myocardium tissue to couple with surrounding cells. Moreover, some of the obtained materials lack fibrous and anisotropic structure, appropriate morphology (porosity, for example, allows oxygen exchange, which it's essential for cardiac construction), and show inadequate degradation rate, low mechanical strength, and poor hydrophilicity (Heidari et al., 2019).

Conductive polymeric/graphene nanocomposites could influence and enhance the electrical conduction and mechanical properties of polymeric nanofibers (Bahrami et al., 2019) without any graphene addition. Hence, conductive polymeric nanofibrous scaffolds are a promising solution for heart failure and broken hearts (Qasim et al., 2019) and some other applications such as nerve, osteoblast, or culture and differentiate stem cells. The aim of this study was comparing the properties of a polymeric scaffold with and without graphene made with nanofibers by electrospinning technique.

Paper Received: 3 February 2022; Revised: 24 March 2022; Accepted: 27 April 2022
Please cite this article as: Munoz-Gonzalez A.M., Clavijo-Grimaldo D., 2022, Synthesis and Characterization of Graphene-doped Nanofibrous Scaffolds for Tissue Engineering, Chemical Engineering Transactions, 94, 1423-1428 DOI:10.3303/CET2294237

2. Materials and Methods

2.1 Materials

Policaprolactone (PCL) (Sigma-Aldrich, CAS # 134490-19-0 MW=80000 Da), polyvinylpirrolidone (PVP) powder (Sigma-Aldrich, CAS # 9003-39-8 MW=10000 Da), ethanol (Sigma-Aldrich, CAS 64-17-5), isopropyl alcohol (Sigma Aldrich, 99,7 % CAS # 67-66-3), chloroform (Sigma Aldrich, 99,5 %, CAS # 67-66-3) and graphene nanoplatelets was purchased in Bravecount Materials, China (CAS # 7782-42-5).

2.2 Polymeric suspensions preparation

For the multi-layer scaffolds obtention by means of the electrospinning technique, it was necessary to prepare:

- PCL suspension: PCL suspension was used at 9% (w/v) in a 50:50 (v/v) chloroform and isopropanol solution. PCL suspension was subjected to an ultrasonic bath (ATU- ATM40-2LCD) with a frequency of 50 Hz per 60 min at 20 °C.
- PVP suspension doped with graphene: PVP was used at 25% (w/v) in 50:50 (v/v) ethanol and water. Afterwards, pristine graphene nanoplatelets solution was added drop by drop at 1% (w/v). PVP with graphene dispersion was stirred in a magnetic stirrer per 60 minutes at room temperature (21 °C). An ultrasonic processor for low volume applications (Cole-Palmer # EW-04714-53) was used to overcome the agglomeration of the graphene nanoplatelets.

2.3 Multilayer fabrication by electrospinning and electrospray process and characterization

The fibers were developed into a vertical electrospinning equipment composed by a high voltage source (CZE1000R, Spellman), a dosing pump (KDS100), a syringe, a needle (gauge 21) and a rotary collector (ESD30s). The distance between needle and rotatory collector was maintained in 15 cm. Applied voltage and solution feed rate was chosen as the most relevant electrospinning parameters and were established until uniform and defect-free fibers were obtained.
The PCL suspension was deposited for 45 min at 1.0 ml/h and 14 kV (first layer, nPCL). The graphene-doped PVP suspension was deposited on the nPCL layer for 30 min at 1.5 ml/h and 23 kV (second layer, PVP+G). A final layer of nPCL was deposited under the same conditions as the first layer to seal the PVP+G. This final multi-layer scaffold was named MLS1. To compare the influence of the graphene layer, a control scaffold without graphene was fabricated using the same conditions mentioned above, this sample was named MLS0 (Figure 1). The process was performed at 21 °C room temperature and 55% RH.

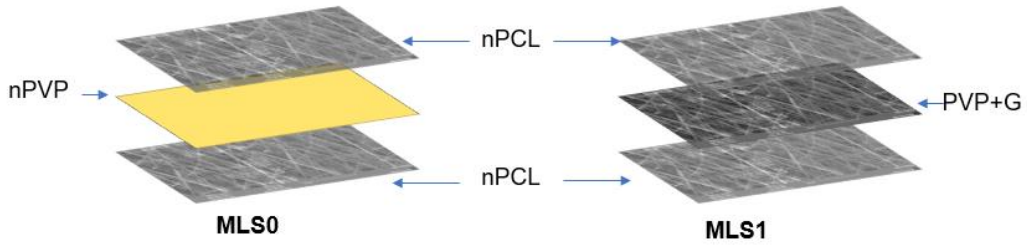

Figure 1 Configuration of MLS0 and MLS1.

The obtained nanofibers was visualized via scanning electron microscopy (SEM) (Tescan Vega 3 SB) at an accelerating voltage of 15 kV. Based on the SEM images, fiber diameter distribution was determined using Image J software. Statistical analysis was performed for determining the mean diameter and standard deviation at least 100 measurements. The conductivity of each suspension was measured (n=3) using a conductivity sensor (Hanna Instruments HI 5522). Measurements was taken at 17 °C. The mechanical properties of the multilayer scaffold were determined by tensile testing technique (Shimadzu UH-I) with 50 N load capacity of 50 mm/min. Procedure and samples were prepared in rectangular-shape pieces with a length of 120 mm and width of 10 mm, according with the ASTM D882. Five specimens were tested to obtain average values. FTIR spectra were obtained with a Shimadzu® FT-IR solutions spectrometer with attenuated total reflectance (ATR) module and germanium crystal. FTIR spectra were recorded in the transmittance mode in the range of 4000 – 500 cm^{-1} and processed with IR Solutions software at environmental temperature conditions.

3. Results and discussion

SEM micrographs of nPCL, nPVP, PVP+G and multilayered scaffolds MLS0 and MLS1 are shown in Figure 2. From the images, it can be observed that the fibers, except in PVP+G exhibited a smooth and bead-free surface that was distributed aligned over the scaffold structure. Figure 3 shows the mean fiber diameter of the nPCL sample was (620.30 ± 168.42) nm, for the PVP sample was (435.86 ± 151.15) nm and for the PVP+G was (371.42 ± 152.18) nm. According to the results, PVP+G reached a smaller diameter than nPVP and even smaller than nPCL, this could be explained because graphene increases the conductivity of the polymeric suspension making the diameter smaller by the increase in the charge transport (Das et al., 2013) and contributing with the stretching and elasticity of the fibers. The size reduction of the diameter is a desirable effect as a lower diameter fiber possesses higher surface area for cell attachment and proliferation (Leung Ko, 2011) . Despite the decrease in the diameter due to the graphene addition, there are beads along the fibers produced by the difficulty of dispersing the graphene. Other results indicated that the percentage used in PCL/Gelatin/graphene fiber (1%) shows beads caused by the overdispersion of graphene (Chen et al., 2019). Further studies with different graphene proportions in polymer suspension and its electrospinning parameters will be addressed to the use of pristine graphene with PVP for tissue engineering applications.

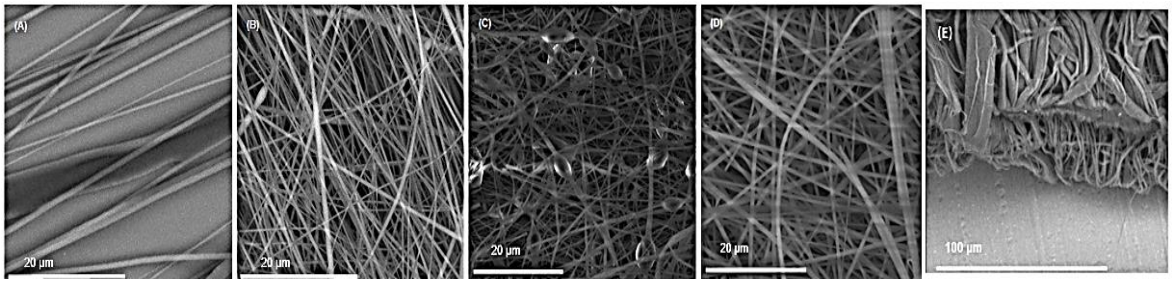

Figure 2 Morphology observed by SEM of (A) nPCL, (B) nPVP, (C) PVP+G, (D) MLS1 surface, and (E) MLS1 thickness.

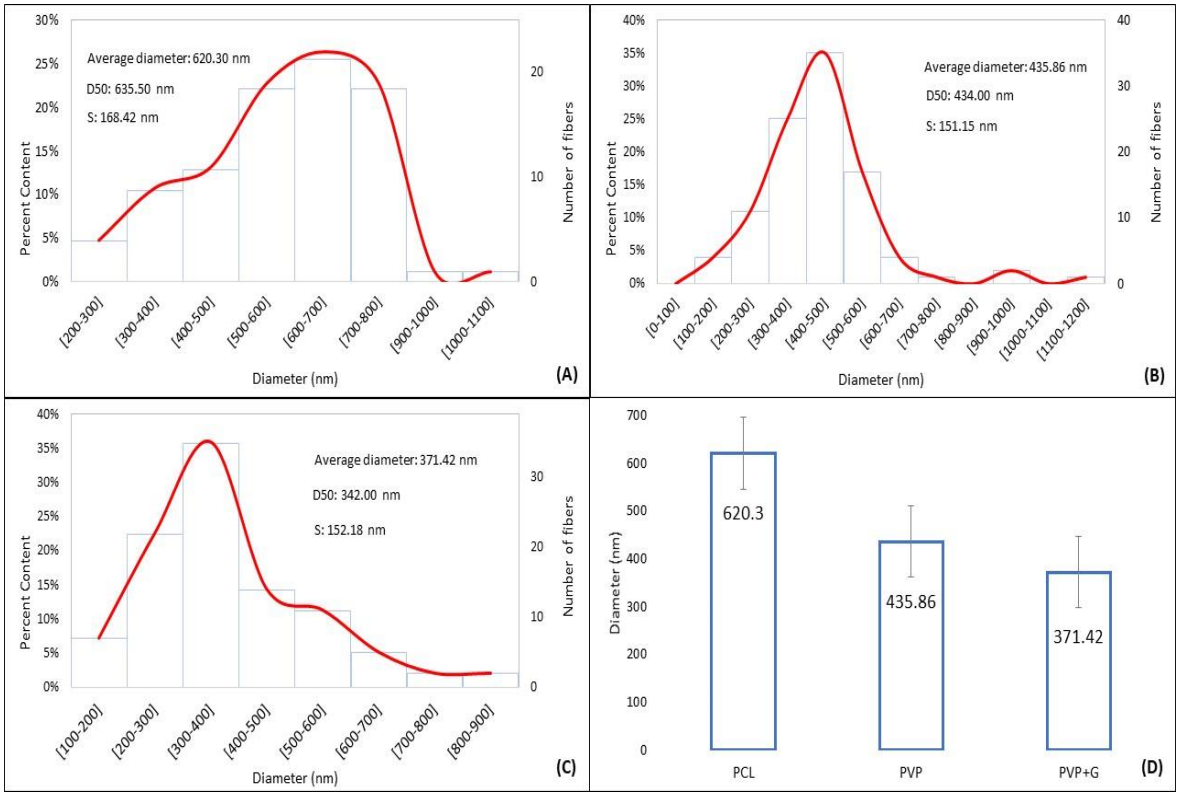

Figure 3 Fiber diameter distributions of (A) nPCL in the MLS0, (B) nPVP, (C) PVP+G and, (D) average diameters summary. D50 is diameter when the cumulative percentage reaches 50% and S is the standard deviation.

Young's modulus, maximum load, and maximum elongation of the scaffolds are presented in Figure 4. The Young's modulus were determined to be 11.65±7.06 MPa, 138.52±6.87 MPa, 33.75±15.99 MPa, and 34.43±7.90 MPa for the nPCL membrane, PVP+G, MLS0, and MLS1, respectively (Figure 4A). In particular, the modulus of MLS0, compared to MLS1 were not significantly different ($p>0.05$). Pure nPCL was the lowest value for Young's modulus because it was not reinforced and slimmer than the other samples. Further, PVP+G had the highest value Young's modulus despite its thickness, mechanical fragility, and lower diameter as shown in Figure 2. In Figure 5 the results show that it is evident the graphene addition reinforces the tensile strength of the polymer matrix.

Other authors with similar material compositions presented similar values. Zhao et al. developed silk biomaterials using controllable surface deposition on the nanoscale to recapitulate electrical microenvironments for cardiac tissue engineering reaching 12-13 MPa in tensile tests (Zhao, G, 2018). In the same way, Liu and Xu got values between 10-60 MPa getting with core-sheath fibers loaded with 5% carbon nanotubes (Liu & Xu, 2017). Obtained results demonstrate an enhancement in mechanical properties due to graphene addition and the improving of multilayer configuration with respect to a single polymer nanofiber scaffold. The obtained values overcome physiological values, so the fabricated material could endure under cyclic stretch due to the rhythmic heartbeat and diastolic and systolic contractions into physiological conditions (Nguyen-truong & Li, 2020).

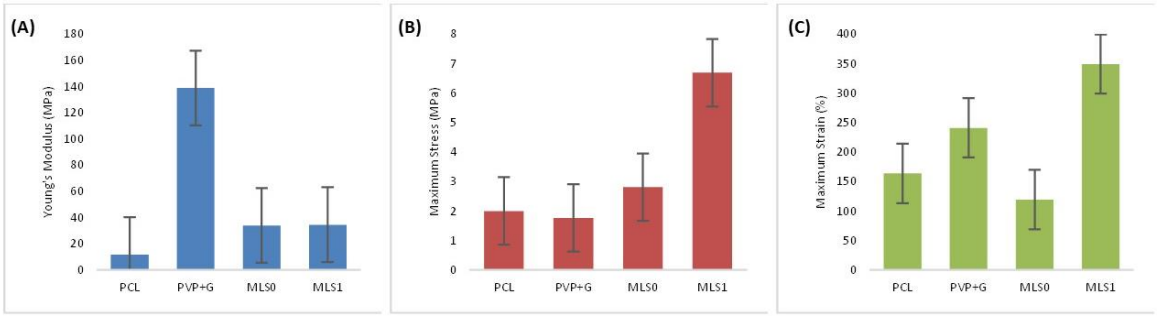

Figure 4 Mechanical properties of nPCL membrane, PVP+G, MLS0 and MLS1. The columns represent (A) Young's Modulus, (B) maximum stress, and (C) maximum strain.

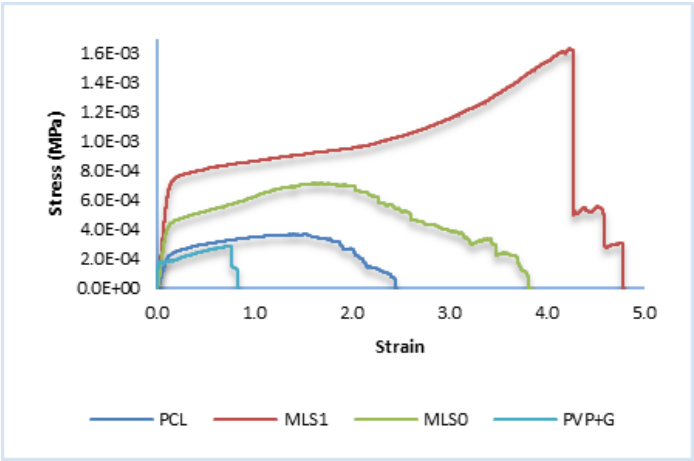

Figure 5 Stress-Strain profiles of a representative sample of the nPCL, PVP+G, MLS0 and MLS1 groups.

Figure 6 represents FTIR spectra of PCL, PVP+G and MLS1 scaffold. Characteristics bands of nPCL were identified at 2945, 2868, 1725, 1291, 1239, and 1170 cm^{-1} and attributed to asymmetric $v_{as}(CH_2)$, symmetric v_s (CH_2) stretching, carbonyl (C=O) stretching, C-O and C-C stretching, asymmetric C-O-C stretching, and symmetric C-O-C stretching, respectively. The FTIR spectra of PVP doped with graphene showed bands at 3431, 2954, 1646, 1373, 1287, 1018, 937, and 841 cm^{-1} corresponding to O-H band, asymmetric $v_{as}(CH_2)$ of pyrrole ring, C=O band, C-H band, CH_2 wagging v(C-N), C-C, C-C bond and $\delta(CH_2)$, respectively, characteristics of PVP. Further, there are peaks at 1460, 1422, 1317,1222 and, 1044 cm^{-1} attributed to CH_2 bending, C-O, δ (CN), v(O-H or Ar-OH) and, C-O alkoxy stretching vibrations may be due to the remaining carbonyl groups after the reduction in the fabrication process of graphene. No presence of the O-H group (3000 and 2500 cm^{-1}), characteristic of the graphene oxide and not of the graphene was detected (Ojrzynska et al., 2020).

All the characteristic peaks of PCL and PVP were identified in the MLS1 scaffold at 2945, 2864, 1725, 1295, 1239, 1165, and 932 cm^{-1}, confirming the structure of the PCL and PVP. Also, peaks at 1417, and 1365 cm^{-1} corresponding to C-O, and δ/β(O–H or C–OH) were observed and are associated with graphene. nPCL, PVP+G and MLS1 curves shown in Figure 6 exhibit, presumably, the interaction between layers by the interaction enclosed by nearby peaks and the similar curves; for example, in 1365 cm^{-1} peak in MLS1 exists an interaction between C-OH in graphene and C-H in PVP.

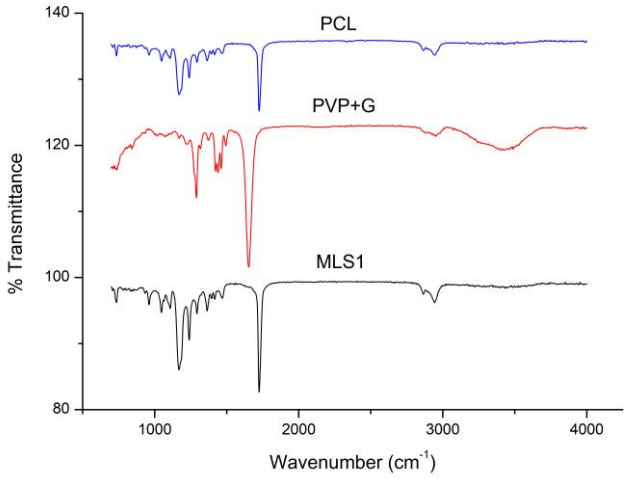

Figure 6 FTIR of (A) nPCL, (B) PVP+G and, (C) MLS1.

PCL, PVP, and PVP+G solutions conductivity were measured. Results were 0.101±0.018, 83.365±0.592 and, 85.867±0.860 µS/cm for PCL, PVP, and PVP+G, respectively. As observed, the PCL solution is insulating because of its low conductivity value. An increase of conductivity by the addition of graphene in PVP solution is satisfactory considering that the nanofiller is graphene rather than graphene oxide. Conductivity value in PVP+G contributes to low diameters as discussed above. As long as the graphene/polymer ratio is low, is possible that the critic point of percolation threshold is not reached maybe because of the viscosity, concentration, or time of preparation of the PVP solution that could affect the graphene dispersion having dead zones where particles can arrive, leaving no interaction with the polymer.

4. Conclusion

The results of this study demonstrate that doping graphene into polymeric nanofibers resulted in the enhancement of morphological properties such as diameter which was smaller than the polymeric mats without graphene despite the appearance of the beads. Tensile measurements showed that graphene can reinforce the mats and it was demonstrated that the effect of the nPCL layer increases the overall mechanical strength of the MLS1 compound and Young's module was higher and overcome the physiological values. FTIR results confirm the chemical composition of the MLS1 scaffold showing probable interactions between graphene and the polymers. It was demonstrated that the doped polymeric solution with graphene improves the electric conductivity even in a low amount. This study is the initial basis of characterization for an appropriate platform to have cell adhesion, proliferation, and an environment to maintain cell viability for use in cardiac engineering tissue.

Acknowledgments

This work develops the first part of the project "Conductive polymeric nanofibers: fabrication, characterization and evaluation of electromechanical coupling in myocardial tissue" founded by the Universidad Nacional de Colombia and the Fundación Universidad Sanitas (Internal Research Call 2021-1). Authors express their acknowledgment to the Electrospray and Electrospinning Laboratory of the Universidad Nacional de Colombia for the space for developing this paper.

References

Ahadian S., Zhou Y., Yamada S., Estili M., Liang X., Nakajima K., Shiku H., Matsue T. (2016). Graphene induces spontaneous cardiac differentiation in embryoid bodies. *Nanoscale*, *8*(13), 7075–7084. https://doi.org/10.1039/c5nr07059g

Bahrami S., Solouk A., Mirzadeh H., Seifalian A. M. (2019). Electroconductive polyurethane/graphene nanocomposite for biomedical applications. *Composites Part B: Engineering*, *168*(March), 421–431. https://doi.org/10.1016/j.compositesb.2019.03.044

Barba Evia J. R. (2009). Cardiomioplastia: El papel de las células madre en la regeneración miocárdica. *Revista Latinoamericana de Patología Clínica y Medicina de Laboratorio*, *56*(1), 50–65.

Chem G., Thomas M. S., Pillai P. K. S., Farrowc S. C., Pothan L. A., Thomas, S. (2021). *Electrospinning as an Important Tool for Fabrication of Nanofibers for Advanced Applications — a Brief Review*. *Figure 1*, 1–7. https://doi.org/10.21127/yaoyigc20200022

Chen X., Feng B., Zhu D. Q., Chen Y. W., Ji W., Ji T. J., Li F. (2019). Characteristics and toxicity assessment of electrospun gelatin/PCL nanofibrous scaffold loaded with graphene in vitro and in vivo. *International Journal of Nanomedicine*, *14*, 3669–3678. https://doi.org/10.2147/IJN.S204971

Das, S., Wajid, A. S., Bhattacharia, S. K., Wilting, M. D., Rivero, I. V., Green, M. J. (2013). Electrospinning of polymer nanofibers loaded with noncovalently functionalized graphene. *Journal of Applied Polymer Science*, *128*(6), 4040–4046. https://doi.org/10.1002/app.38694

Fleischer S., Feiner R., Dvir T. (2017). Cardiac tissue engineering: From matrix design to the engineering of bionic hearts. *Regenerative Medicine*, *12*(3), 275–284. https://doi.org/10.2217/rme-2016-0150

Heidari M., Bahrami H., Ranjbar-Mohammadi, M. (2017). Fabrication, optimization and characterization of electrospun poly(caprolactone)/gelatin/graphene nanofibrous mats. *Materials Science and Engineering C*, *78*, 218–229. https://doi.org/10.1016/j.msec.2017.04.095

Heidari M., Bahrami S. H., Ranjbar-Mohammadi M., Milan, P. B. (2019). Smart electrospun nanofibers containing PCL/gelatin/graphene oxide for application in nerve tissue engineering. *Materials Science and Engineering C*, *103*(May), 109768. https://doi.org/10.1016/j.msec.2019.109768

Karkan S. F., Davaran S., Rahbarghazi R., Salehi R., Akbarzadeh A. (2019). Electrospun nanofibers for the fabrication of engineered vascular grafts. *Journal of Biological Engineering*, *7*, 1–13.

Kharaziha M., Shin S. R., Nikkhah M., Topkaya S. N., Masoumi N., Annabi N., Dokmeci M. R., Khademhosseini A. (2014). Tough and flexible CNT-polymeric hybrid scaffolds for engineering cardiac constructs. *Biomaterials*, *35*(26), 7346–7354. https://doi.org/10.1016/j.biomaterials.2014.05.014

Leung V., Ko F. (2011). Biomedical applications of nanofibers. *Polymers for Advanced Technologies*, *22*, 350–365. https://doi.org/10.1002/pat.1813

Liu H., Paul C., Xu M. (2017). Optimal environmental stiffness for stem cell mediated ischemic myocardium repair. *Adult Stem Cells*, 293–304.

Nguyen-truong M., Li Y. V. (2020). *Mechanical Considerations of Electrospun Sca ff olds for Myocardial Tissue and Regenerative Engineering*. 1–22.

Ojrzynska M., Wroblewska A., Judek J., Malolepszy A., Duzynska A., Zdrojek M. (2020). Study of optical properties of graphene flakes and its derivatives in aqueous solutions. *Optics Express*, *28*(5), 7274. https://doi.org/10.1364/oe.382523

Qasim M., Arunkumar P., Powell H. M., Khan M. (2019). Current research trends and challenges in tissue engineering for mending broken hearts. *Life Sciences*, *229*(March), 233–250. https://doi.org/10.1016/j.lfs.2019.05.012

Randviir E. P., Brownson D. A. C., Banks C. E. (2014). A decade of graphene research: Production, applications and outlook. In *Materials Today* (Vol. 17, Issue 9, pp. 426–432). Elsevier. https://doi.org/10.1016/j.mattod.2014.06.001

Ratih D., Siburian R., Andriayani. (2018). The performance of graphite/n-graphene and graphene/n-graphene as electrode in primary cell batteries. *Rasayan Journal of Chemistry*, *11*(4), 1649–1656. https://doi.org/10.31788/RJC.2018.1145007

Ţucureanu, V., Matei A., Avram A. M. (2016). FTIR Spectroscopy for Carbon Family Study. *Critical Reviews in Analytical Chemistry*, *46*(6), 502–520. https://doi.org/10.1080/10408347.2016.1157013

Xue J., Wu T., Dai Y., Xia Y. (2019). Electrospinning and electrospun nanofibers: Methods, materials, and applications. *Chemical Reviews*, *119*(8), 5298–5415. https://doi.org/10.1021/acs.chemrev.8b00593

Ye G., Qiu X. (2017). Conductive biomaterials in cardiac tissue engineering. *Biotarget*, *1*(5), 9–9. https://doi.org/10.21037/biotarget.2017.08.01

Zhao G., Qing H., Huang G., Genin G. M., Lu T. J., Luo Z., Xu F., Zhang X. (2018). Reduced graphene oxide functionalized nanofibrous silk fibroin matrices for engineering excitable tissues. *NPG Asia Materials*, *10*(10), 982–994. https://doi.org/https://doi.org/10.1038/s41427-018-0092-8